Supplement of Biogeosciences, 13, 3021–3034, 2016
http://www.biogeosciences.net/13/3021/2016/
doi:10.5194/bg-13-3021-2016-supplement

Biogeosciences Open Access EGU

Supplement of

Transfer of radiocaesium from contaminated bottom sediments to marine organisms through benthic food chains in post-Fukushima and post-Chernobyl periods

Roman Bezhenar et al.

Correspondence to: Vladimir Maderich (vladmad@gmail.com)

Supplementary materials to the paper "Transfer of radiocaesium from contaminated bottom sediments to marine organisms through benthic food chain"

Poseidon-R model

The mechanisms of radionuclide transfer in the POSEIDON-R model (Lepicard et al., 2004) are as follows. Activity entering the water column is transported by currents and turbulent diffusion and lost to bottom sediments through sorption on suspended particles which then settle out. The exchange of activity between the upper layer of the sediment and the water column is described as diffusion and bioturbation (modelled as a diffusion process). Activity in the upper sediment layer may diffuse downward but there is also an effective downward transfer via the continued sedimentation at the top of the sediment layers. Return of activity from the middle sediment to the top sediment occurs only through diffusion. The effective loss of activity from middle sediment to deep sediment arises from the continued deposition of sediment. A more detailed composition of the water column and its sediment layers, as well as its interaction with neighbouring volumes is shown in Fig. S1.

The POSEIDON-R equations are obtained by averaging the three dimensional transport equations for the dissolved radionuclide concentration C_w (Bq·m^{-3}) and the concentration in the three layers of the bottom sediment. It is assumed that the activity in the water column is partitioned between the water phase and the suspended sediment material, resulting in the following relation:

$$C_{ss} = K_d C_w . \tag{S1}$$

where C_{ss} (Bq·kg^{-1}) is the concentration of radioactivity sorbed by suspended sediment, K_d is the radionuclide distribution coefficient (m^3·kg^{-1}). The equations read as follows.

For the water column layers:

$$\frac{\partial C_{w,i}}{\partial t} = \sum_j \left[\frac{F_{ji}}{V_{w,i}} C_{w,j} - \frac{F_{ij}}{V_{w,j}} C_{w,i} \right] + \gamma_{0i} C_{w,(i,j,k-1)} - (\gamma_{1i} + \lambda) C_{w,i} + \frac{L_{t,i}}{h_i} \gamma_2 C_{s,1} + Q_{si}; \tag{S2}$$

for the upper sediment layer:

$$\frac{\partial C_{s,1}}{\partial t} = -(\gamma_2 + \gamma_3 + \lambda) C_{s,1} + \frac{h_i}{L_{t,i}} \gamma_{1,i} C_{w,i} + \frac{L_{m,i}}{L_{t,i}} \gamma_4 C_2, ; \tag{S3}$$

for the middle sediment layer:

$$\frac{\partial C_{s,2}}{\partial t} = -(\gamma_4 + \gamma_5 + \lambda) C_{s,2} + \frac{L_{t,i}}{L_{m,i}} \gamma_3 C_{s,1}. \tag{S4}$$

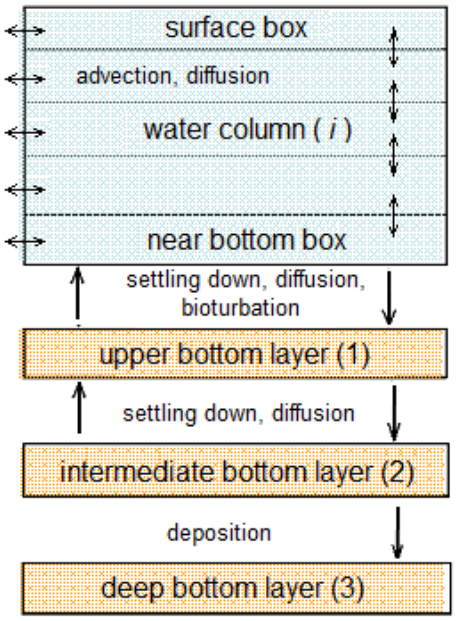

Fig.S1 Vertical structure and radionuclide transfer processes in the compartment of POSEIDON-R model. Arrows show exchange between boxes and layers.

Here subscript (0) denotes the water column, subscripts (1) and (2) denote the upper and middle sediment layer, respectively; $C_{w,i}$ is the box averaged concentration of radionuclide C_w in the water column layer i; $C_{s,1}$ is the averaged concentration of radionuclide in the upper sediment layer; $C_{s,2}$ is the averaged concentration in the middle sediment layer; λ (y^{-1}) is the radionuclide decay constant; F_{ij} is the water flux ($t \cdot y^{-1}$) from box i to box j; $V_{w,i}$ is the box volume (m^3); h_i is the depth of the water box layer (m); L_t, L_m are the depth (m) of top and middle bottom sediment layers respectively; Q_{si} is the point source of the activity in box i (Bq y^{-1}); $\gamma_0 \ldots \gamma_5$ are the coefficients, their values depend on the characteristics of the radionuclide and sediments.

For the surface water layer, the coefficients are as follows:

$$\begin{aligned} \gamma_{0i} &= 0, \\ \gamma_{1i} &= \frac{K_d SSW}{h_i(1+K_d SS)}, \\ \gamma_2 &= 0. \end{aligned} \tag{S5}$$

and for the layers in the water column below the surface water layer, the coefficients are defined as follows:

$$\begin{aligned} \gamma_{oi} &= \frac{K_d SSW}{h_i(1+K_d SS)}, \\ \gamma_{1i} &= \frac{K_d SS}{h_i(1+K_d SS)}, \\ \gamma_2 &= 0. \end{aligned} \tag{S6}$$

In the near bottom layer located at the bottom of the water column just above the bottom sediment, the coefficients are defined as:

$$\gamma_{oi} = \frac{K_d SSW}{h_i(1+K_d SS)},$$

$$\gamma_{1i} = \frac{K_d SSW}{h_i(1+K_d SS)} + \frac{1}{(1+K_d SS)} \frac{1}{L_b \min(L_b, L_t)} + \frac{K_d SSW}{(1+K_d SS)} \frac{B}{L_b \min(L_b, L_t)},$$

$$\gamma_2 = \frac{1}{R} \frac{D}{L_t \min(L_b, L_t)} + \frac{(R-1)}{R} \frac{B}{L_t \min(L_b, L_t)},$$

$$\gamma_3 = \frac{R-1}{R} \frac{SSW}{L_t(1-\varepsilon)\rho} + \frac{1}{R} \frac{D}{L_t \min(L_t, L_m)},$$

(S7)

$$\gamma_4 = \frac{1}{R} \frac{D}{L_m \min(L_t, L_m)},$$

$$\gamma_5 = \frac{(R-1)}{R} \frac{SSW}{L_m(1-\varepsilon)\rho},$$

where the coefficient R is defined as:

$$R = 1 + \frac{\rho(1-\varepsilon)}{\varepsilon} K_d \quad \text{(S8)}$$

Here L_b (m) is the length scale of the bottom boundary layer, SS is the different for each box concentration of suspended sediments ($t \cdot m^{-3}$), obtained from observations or model simulation, W_g is the settling velocity calculated as a function of suspended particles size; $SSW = SS \cdot W_g$ is the fixed sediment flux ($t \cdot m^{-2} \cdot yr^{1}$); D is the coefficient of vertical diffusion in the bottom; B is the coefficient of bioturbation in the top bottom; ε is the porosity of the bottom sediment; ρ is the sediment density.

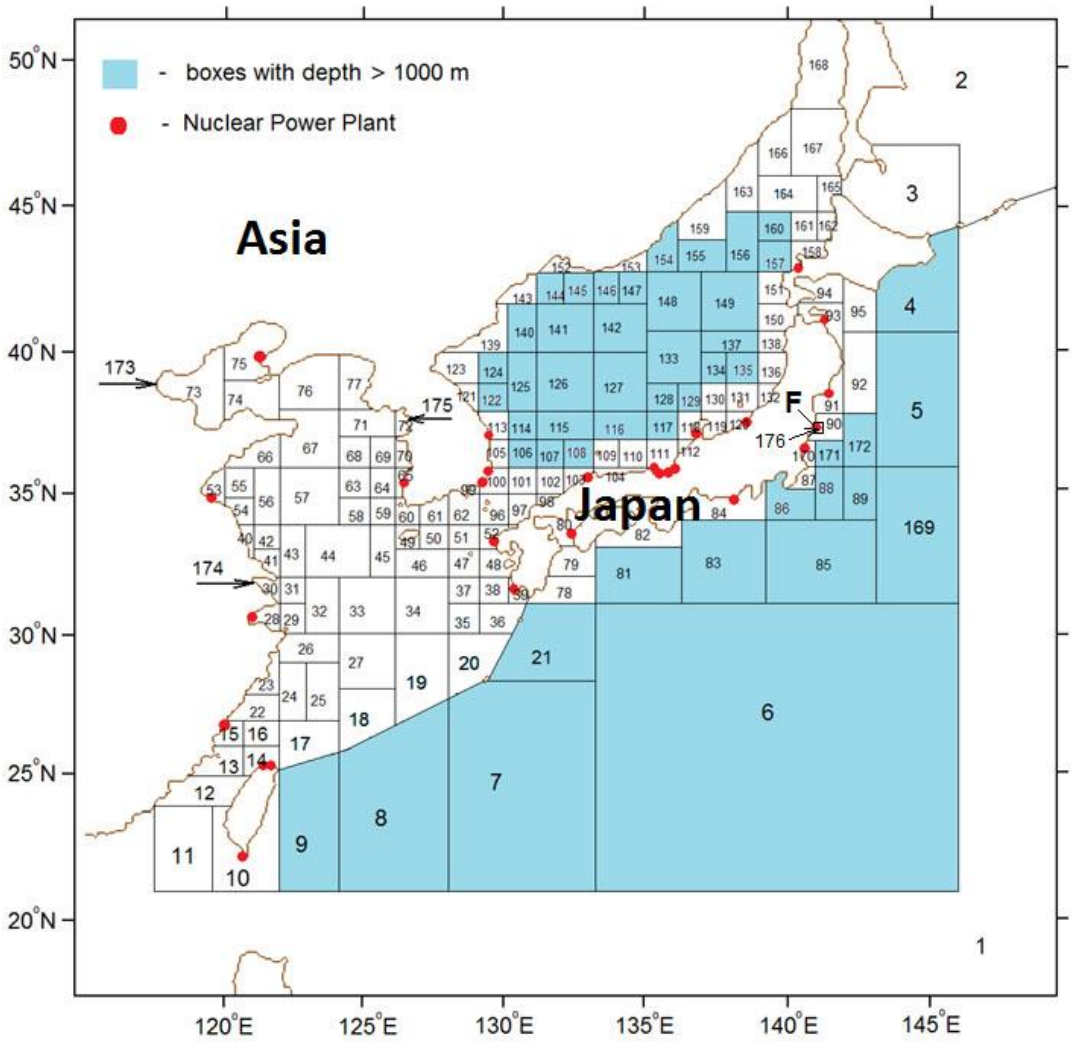

Fig. S2. The compartment system for the Northwestern Pacific. The shaded boxes represent the deep water boxes. The arrows with numbers show the compartments representing estuaries of large rivers (174 – the Yangtze River, 173 – the Huanghe River and 175 – the Han River. The NPPs are shown by filled circles. Letter “F” represent the Fukushima Dai-ichi NPP.

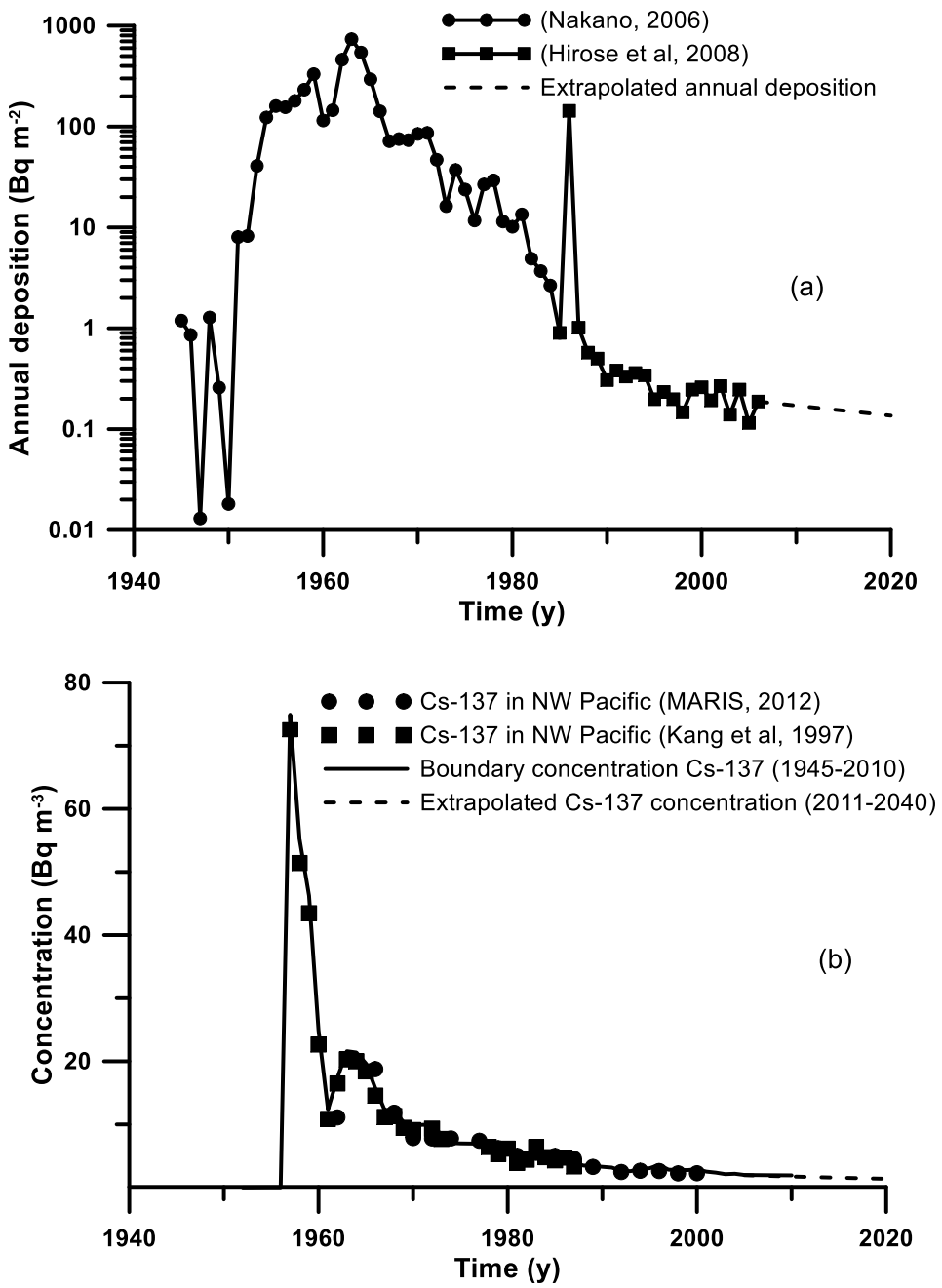

Fig. S3. Time variations of the annual deposition on the surface compiled from Nakano (2006) and Hirose et al (2008) (a) and the boundary values for the ^{137}Cs concentration in the NW Pacific compiled from MARIS (2012) database and Kang et al. (1997) (b).

Table S1 The model parameters for coastal box around the FDNPP and box 45 in the Baltic Sea.

Parameter	Coastal box (Fukushima case)	Box 45 (Baltic Sea case)
Volume, km^3	22.5	776.3
Average depth, m	50	31.4
Water exchange rate with adjacent compartments, $km^3 yr^{-1}$	150	4430
Thickness of top sediment layer, m	0.1	0.05
Concentration of suspended sediments, kg/m^3	$8 \cdot 10^{-2}$	$1 \cdot 10^{-3}$
Sedimentation rate, $kg(m^2\ yr)^{-1}$	$1 \cdot 10^{-2}$	$7.5 \cdot 10^{-2}$
Salinity, PSU	35	15
Sediment density, $kg\ m^{-3}$	2600	2600
Vertical diffusion coefficient in bottom sediments, $m^2 yr^{-1}$	$3.15 \cdot 10^{-2}$	$3.15 \cdot 10^{-2}$
Bioturbation coefficient, $m^2 yr^{-1}$	$3.6 \cdot 10^{-5}$	$3.6 \cdot 10^{-5}$
Porosity of bottom sediments	0.75	0.75
^{137}Cs distribution coefficient, K_d, $m^3 \cdot kg^{-1}$	2	2

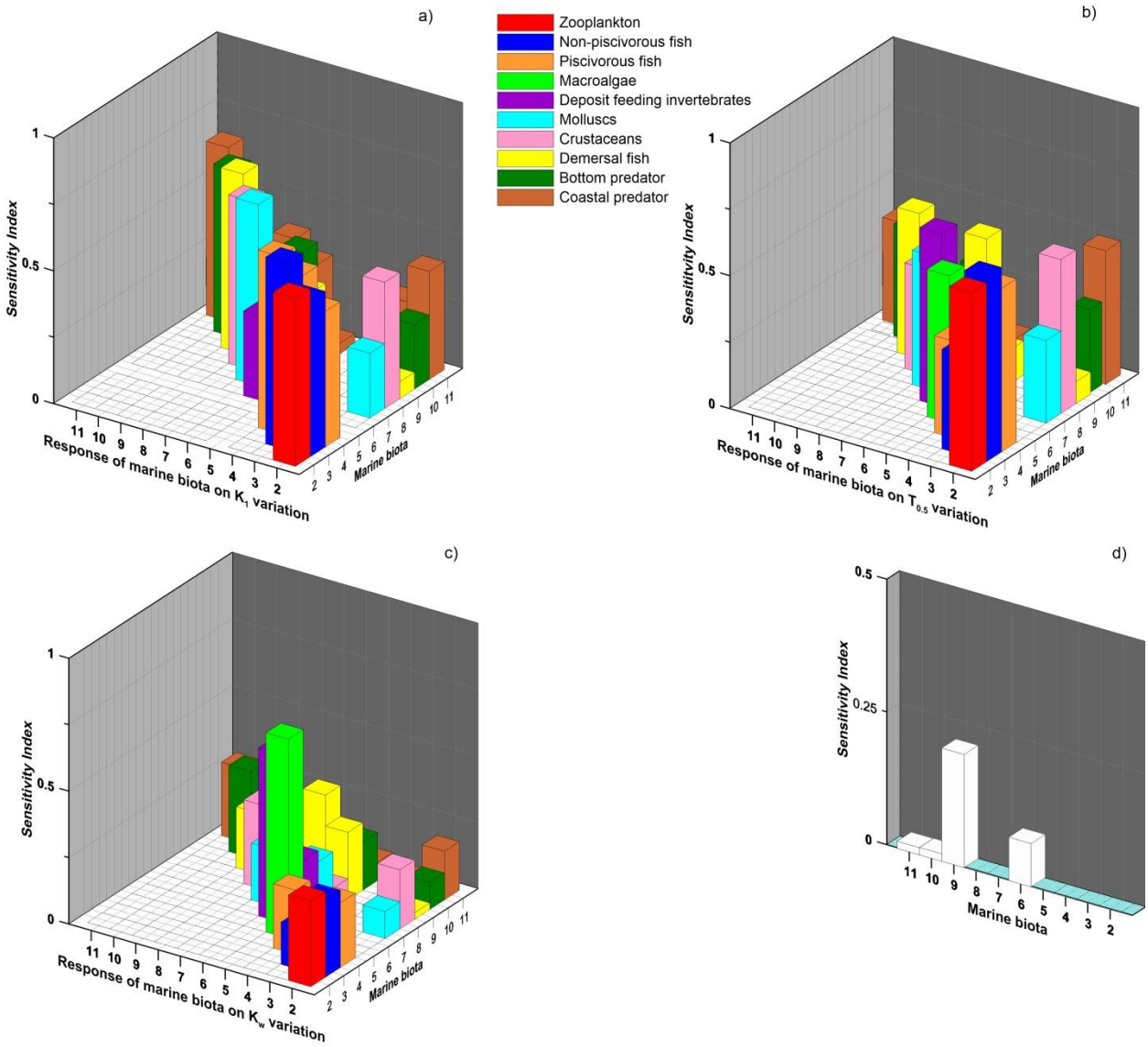

Fig. S4. Sensitivity indexes calculated for food uptake rate K_1 (a), biological half-life $T_{0.5}$ of ^{137}Cs in the organism (b), water uptake rate K_w (c) and for ratio of concentration of assimilated radioactivity from organic fraction of bottom sediment to the concentration of radioactivity of bulk bottom sediment ϕ_{org} (d).

Table S2 The river runoff into the Baltic Sea (Lepparanta and Myrberg, 2009.

River box → Baltic Sea box	Rivers	Inflow ($km^3 \cdot yr^{-1}$)
82 → 36	Gota-alv + small rivers	23
83 → 39	All Danish rivers	5
84 → 43	Small German rivers	9
85 → 45	Oder + small rivers	25
86 → 47	Wisla + small rivers	50
87 → 48	Neman + small rivers	30
88 → 59	Motala strem + Swedish small rivers	9
89 → 58	Daugava + small rivers	31
90 → 65	Narva + small rivers	20
91 → 66	Kymijoki + small rivers	13
92 → 67	Neva	79
93 → 71	Dalalven + small rivers	18
94 → 77	Kokemenjoki + other Finnish small rivers	25
95 → 78	Angerman-alv + Indals-alv + smaller rivers	47
96 → 80	Ume-alv + smaller rivers	22
97 → 81	Kemijoki + Oulujoki + Lijoki + Torne-alv + Kalix-alv + Lule-alv + smaller rivers	78

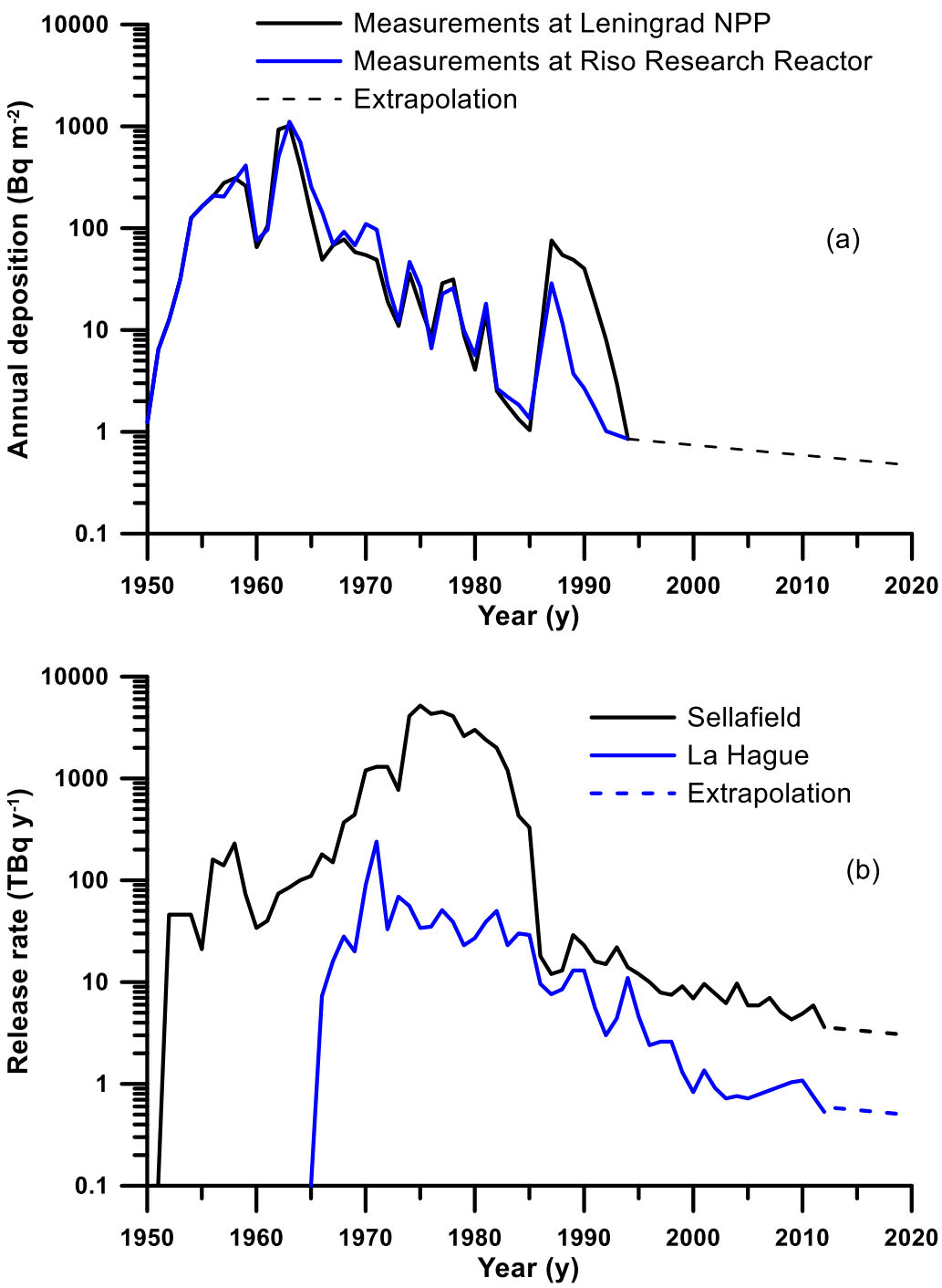

Fig. S5. Global atmosphere deposition rate of ^{137}Cs on the Baltic Sea (HELCOM, 1995) (a) and release of ^{137}Cs from Sellafield and La Hague reprocessing plants (HELCOM, 2009).

Table S3. Atmosphere deposition density of ^{137}Cs in 1986 due to the Chernobyl accident (HELCOM, 1995)

Basin	Deposition density, Bq m^{-2}	Inventory, PBq	Boxes
North-Atlantic	1000	35.4	3-34
Kattegat	1700	0.04	35-40
Belt Sea	1800	0.05	41-43
Baltic Proper	4500	0.82	44-57, 59-61
Gulf of Riga	5000	0.08	58
Gulf of Finland	15000	0.83	62-67
Aland Sea	72500	0.55	68-69, 71-72
Archipelago Sea	17300	0.04	70
Bothnian Sea	35000	1.94	73-79
Bothnian Bay	6900	0.31	80-81